Astron. Astrophys. 73, 67–73 (1979)

ASTRONOMY AND ASTROPHYSICS

A Monte Carlo Approach to Non-LTE Radiative Transfer Problems

C. Bernes

Stockholms Observatorium, S-13300 Saltsjöbaden, Sweden

Received May 25, revised August 10, 1978

Summary. A procedure for the solution of non-LTE, multi-level, radiative transfer problems using the Monte Carlo method is developed and shown to be useful. This procedure allows the inclusion of velocity fields, inhomogeneities and complex geometries. It is applied to a study of the transfer of CO line radiation in a model of a spherical, collapsing dark cloud. A technique for reducing the random fluctuations inherent in the Monte Carlo method is introduced. This technique typically cuts down computing times by an order of magnitude in the investigated case. Line profiles accurate to 1% or better were obtained with a very reasonable amount of computing time.

Key words: radiative transfer – Monte Carlo methods – dark clouds – interstellar molecules – carbon monoxide

1. Introduction

Conventional numerical methods for solution of multi-level, non-LTE, radiative transfer problems have been developed to a high degree of efficiency and versatility during the past decade, and have to some extent become able to deal with complications like velocity fields and inhomogeneous media. However, this has also brought increased complexity – the sheer size of the computer programs is close to the limits of what both program developers and available computers can manage.

The Monte Carlo method presents a radically different way of approaching the whole problem. Using this method, one can simulate a complex physical situation with a program a fraction of the size of a conventional one. When writing such a program, one is rarely forced away from the physics of the investigated system into intricate numerical considerations. Furthermore, there is virtually no limit to the amount of complications that can be successfully introduced – these include redistribution functions of any kind, velocity gradients of any size, and geometries and inhomogeneities of any degree of complexity. Except possibly for the last one mentioned, none of these complications increases program size or computing time by much, and in neither case is the programming made significantly more difficult.

The main drawback of the method described below is the square-root convergence typical for all Monte Carlo procedures. In general, however, the simplicity of the programs and the modest requirements of memory space make possible the use of an inexpensive minicomputer.

The Monte Carlo method has already been used to solve several radiative transfer problems, and general introductions to the technique are given by Fleck (1963) and House and Avery (1969). Many of the applications deal with scattering in resonance lines (cf. Auer, 1968; Avery and House, 1968; Avery et al., 1969; Caroff et al., 1972; Magnan, 1970 and 1972; Modali et al., 1972 and 1975), but none of these works contains a self-consistent non-LTE analysis or a study of a multi-level system. Fleck (1963) has described a general Monte Carlo procedure for the calculation of non-linear radiative transfer that is well adapted to studies of time-dependent systems. It is similar in some basic respects to the method developed here, but requires more memory space. Fleck did not apply the procedure specifically to line radiation, but noted that this could be done. Price (1969) made an elaborate non-LTE analysis of a pure hydrogen stellar atmosphere, and included continuous opacity sources, but treated the radiation in the lines in a crude way.

The aims of this paper are to demonstrate the simplicity of the Monte Carlo approach to non-LTE, multi-level, radiative transfer problems, and to show that the method is worthy of consideration in studies of line radiation in such regions as extended stellar envelopes and interstellar clouds. The procedure is described in detail in Sect. 2. A technique for variance-reduction is discussed in Sect. 3, and the performance of the Monte Carlo procedure in a simple test case – a study of CO line profiles in a spherical, homogeneous, collapsing dark cloud – is evaluated in Sect. 4. An appendix describes the pseudo-random number generator and how it has been applied. A listing of the computer program has been published separately (Bernes, 1978).

2. The Basic Monte Carlo Procedure

We study the transfer of radiation in a spectral line caused by transitions in two-level atoms (the treatment will, of course, be valid for molecular transitions as well), and the corresponding effects on the populations n_l and n_u per unit volume in the lower and upper energy levels. The scattering in this transition is assumed to be incoherent in direction and frequency, i.e. we assume complete redistribution. Our principal goal is to derive the steady-state values of n_l and n_u.

The fundamentals of the Monte Carlo procedure are as follows: All line photons that are emitted during one second are simulated by a number of model photons, each of which represents a large quantity of "real" photons. These model photons are followed through the region that contains the atoms under study (hereafter simply referred to as "the region"). The number of absorption events caused by the radiation that is represented by a model photon is calculated and stored. As the model photon travels in the region, its weight is continuously modified in order to account for these absorptions and for the stimulated emissions that also may take place. The total number of absorption events

caused by all model photons is used to derive new level populations, and the whole process can then be repeated.

Photons are emitted through excitations to the upper level followed by spontaneous radiative deexcitations. The number N_r of such emissions per unit volume during one second is

$$N_r = n_u A_{ul}, \tag{1}$$

where A_{ul} is the Einstein probability for spontaneous emission.

The region is thought of as consisting of an ensemble of boxes or shells, each with a given kinetic temperature and density. The model photons are emitted at random locations within the boxes. The number of real photons emitted during one second in each box can be derived from the local value of N_r, with some initial estimate of n_u. This determines the relative numbers of model photon emissions in the different boxes. These numbers are not necessarily integers – the fractional parts correspond to emissions of model photons with reduced weights. The total number of real photons emitted within one second also gives the number W_0 of real photons that each model photon represents.

In addition, an exterior radiation field may be dealt with by allowing an appropriate number of model photons to enter the region from the outside. If this radiation field is continuous, the frequency ν_{ul}. We have assumed complete angular redistribution, in a frequency band that covers the line completely.

Each model photon created within the region is emitted in a random direction, represented by the unit vector $\boldsymbol{n}$, and given a random frequency deviation $\Delta\nu$ from the laboratory line centre frequency ν_{ul}. We have assumed complete angular redistribution and the distribution of emission directions is therefore isotropic. The distribution of frequency deviations is defined by a normalized emission profile function $\phi(\nu)$, e.g. the Doppler profile

$$\phi(\nu) = \frac{1}{\sigma\sqrt{\pi}} \exp\left\{-\left(\nu - \nu_{ul} - \boldsymbol{v}\cdot\boldsymbol{n}\,\frac{\nu_{ul}}{c}\right)^2/\sigma^2\right\}. \tag{2}$$

The Doppler width σ is determined by the local kinetic temperature and microturbulence, and the frequency of the actual line centre may be shifted from ν_{ul} by a velocity field, specified by the vector $\boldsymbol{v}$. This velocity field may vary continuously (or, of course, discontinuously) in the whole region.

An emitted model photon is allowed to travel a short distance s_1 in the selected direction, and the coordinates of the new position are calculated. The optical depth τ_1 along the path can be approximated by

$$\tau_1 = \frac{h\nu_{ul}}{4\pi}\,\phi(\nu)\,(n_{l,m}B_{lu} - n_{u,m}B_{ul})\,s_1, \tag{3}$$

where $n_{l,m}$ and $n_{u,m}$ are the level populations in the box (denoted by m) that contains the new position. B_{lu} and B_{ul} are the Einstein probabilities for absorption and stimulated emission (i.e. radiation-induced excitation and deexcitation, respectively). The simplicity of Eq. (3) is partly due to the assumption of complete frequency redistribution, which means that the absorption profile is equal to the emission profile. $\phi(\nu)$ is evaluated at the new position, or taken as a mean of the values at the original and new positions.

The weight $W(x)$ (as a function of the covered distance x) of the model photon, originally taken to be W_0, varies as $W_0 \exp(-\tau_1 x/s_1)$ along the path, and is thus $W_0 \exp(-\tau_1)$ when the distance s_1 is covered.

The model photon induces radiative excitations and deexcitations as it travels from $x=0$ to $x=s_1$. The total number N_{lu} of radiative excitations along this path is

$$N_{lu} = \frac{h\nu_{ul}}{4\pi}\,\phi(\nu)\,n_{l,m}B_{lu}\int_0^{s_1} W(x)\,dx. \tag{4}$$

Since the total number of atoms in the lower state in box m is $n_{l,m}V_m$, where V_m is the volume of the box, the number $S_{lu,m}$ of radiative excitations *per atom in the lower state in box m* caused by this first step of the model photon becomes

$$S_{lu,m} = \frac{N_{lu}}{n_{l,m}V_m} = \frac{h\nu_{ul}}{4\pi}\,\phi(\nu)\,B_{lu}\,\frac{s_1 W_0}{V_m \tau_1}\,\{1-\exp(-\tau_1)\}. \tag{5}$$

This quantity is added to a counter, denoted by $\Sigma\, S_{lu,m}$.

A new step is now taken in the same direction, and the above calculations are repeated. The generalized version of Eq. (5), to be used after step k, is

$$S_{lu,m'} = \frac{h\nu_{ul}}{4\pi}\,\phi(\nu)\,B_{lu}\,\frac{s_k W_0 \exp\left(-\sum_{i=1}^{k-1}\tau_i\right)}{V_{m'}\tau_k}\,\{1-\exp(-\tau_k)\}. \tag{6}$$

The model photon may now be in another box, and this is reflected by the change from index m to index m'. In general, it is advantageous to choose the step lengths so that the steps are taken between those points where the model photon crosses boundaries between different boxes. However, the step length should never be allowed to exceed the distance over which the absorption coefficient at any given frequency changes significantly due to physical density variations or the velocity gradient. The model photon is followed until it escapes from the region or until its weight is small enough to be insignificant. A new model photon is then emitted.

When all model photons have been emitted and followed, we can adjust the level populations in the different boxes, using the common equation of statistical equilibrium:

$$n_l\left\{\frac{B_{lu}}{4\pi}\oint\int_0^\infty I(\nu,\boldsymbol{n})\,\phi(\nu)\,d\nu d\omega + C_{lu}\right\} = n_u\left\{A_{ul} + \frac{B_{ul}}{4\pi}\oint\int_0^\infty I(\nu,\boldsymbol{n})\,\phi(\nu)\,d\nu d\omega + C_{ul}\right\}. \tag{7}$$

C_{lu} and C_{ul} are the rates of collisional excitations and deexcitations per atom, respectively, and $I(\nu,\boldsymbol{n})$ is the specific intensity at frequency ν in the direction $\boldsymbol{n}$.

The first term within the brackets on the left-hand side of Eq. (7) is the rate of radiation-induced excitations (absorptions) per atom in the lower state. But this is the quantity that has been accumulated in the counters $\Sigma\, S_{lu,m}$ for each box m – these counters measure the number of absorptions per atom in the lower state *that have been caused by photons emitted during one second of time.* Similarly, the second term within the brackets on the right-hand side is the rate of radiation-induced deexcitations (stimulated emissions). Since

$$B_{ul} = \frac{g_l}{g_u}\,B_{lu}, \tag{8}$$

where g_l and g_u are the statistical weights of the two levels, this second term can be replaced by $(g_l/g_u)\,\Sigma\, S_{lu,m}$.

The modified version of Eq. (7) then is

$$n_l\{\Sigma\, S_{lu,m} + C_{lu}\} = n_u\left\{A_{ul} + \frac{g_l}{g_u}\,\Sigma\, S_{lu,m} + C_{ul}\right\}, \tag{9}$$

which can be solved using the additional condition that $n_l + n_u = \text{constant}$.

The new values of n_u are used to revise N_r in Eq. (1) for each box. A new series of model photon emissions can now be started. The $\Sigma S_{lu,m}$ counters can be emptied after each such iteration, but it may be more advantageous to continue the accumulation in these counters, since this will bring down the random noise. $\Sigma\, S_{lu,m}$ in Eq. (9) should in that case be replaced by $\Sigma\, S_{lu,m}/\mathcal{N}_{\text{iter}}$, where $\mathcal{N}_{\text{iter}}$ is the number of completed iterations. However, if the initial estimates of the level populations were far off the mark, the radiation field measured by the counters during the first iterations was also far from being correct. It may in such cases be advisable to empty the counters when the level populations after a few iterations have been approximately stabilized, and start over again with the new population values.

The expansion of this procedure to a multi-level case is straightforward. Each radiative transition can be simulated separately by a number of model photon emissions. Alternatively, some computing time may be saved by letting the model photons represent the radiation in all of the transitions simultaneously – only their weights and the contributions to the counters are then calculated separately for each transition. Tests have shown that this alternative can also give a lower random noise than the first one mentioned. When all radiative transitions have been dealt with in one way or the other, the level populations can be adjusted with the use of a generalized form of Eq. (9), and the calculations are then repeated through a number of iterations.

The computing time spent on solving the equations of statistical equilibrium after each iteration is small compared to the total time, as long as the number of involved energy levels is reasonably limited. Hence, the increase with the number of radiative transitions of the computing time necessary to achieve a certain accuracy is approximately linear, or even slower if the alternative procedure described in the previous paragraph is used.

The rate of convergence depends on two factors – (1) the random noise inherent in the Monte Carlo technique and (2) the iterative procedure. The iterations will rapidly bring the *mean* values of the randomly fluctuating level populations near the correct ones if the region is optically thin in all transitions, but the convergence will be slower if the optical depth is great in any transition. The minimum number of iterations that is necessary for convergence is of the same order as the maximum optical depth. This is due to the fact that the model photons cannot carry information about the radiation field and excitation temperature in any part of the region much farther than one optical depth unit per iteration. It should be kept in mind, though, that in typical cases most of the computing time is spent on following the model photons. Thus, 100 iterations consisting of 100 model photon emissions do not take much more time than 10 iterations consisting of 1000 emissions, and the *average* result of a large number of similar runs with different sets of random numbers will be more correct in the former case than in the latter. On the other hand, while the random noise is proportional to $1/\sqrt{\mathcal{N}_{\text{phot}}}$, where $\mathcal{N}_{\text{phot}}$ is the number of model photon emissions during each iteration, it decreases slower than $1/\sqrt{\mathcal{N}_{\text{iter}}}$ even if the accumulation in the counters is continued, since the results of consecutive iterations are not independent of each other. This means that the noise will be greater in the former case as compared to the latter. The noise may, however, in some cases be considerably reduced, as described in Sect. 3.

When one is satisfied with the convergence of the level populations, the spectrum of the radiation that leaves the region in various directions can easily be calculated, since the source function is now considered to be known. The intensity $I_{em}(\nu)$ of the emitted radiation simply is

$$I_{em}(\nu)=I_{bg}(\nu)\exp\{-\tau(X)\}+\int_0^X j(\nu,x)\exp\{-\tau(x)\}\,dx. \tag{10}$$

Here, $I_{bg}(\nu)$ is the specific intensity of the background radiation, $\tau(x)$ is the optical depth from the near surface of the region to the position x along the ray under study, and X is the position where the ray leaves the region on the far side. The emissivity $j(\nu,x)$ at x can be expressed as

$$j(\nu,x)=\frac{h\nu_{ul}}{4\pi}\,\phi(\nu)\,n_{u,m(x)}\,A_{ul}, \tag{11}$$

where the index $m(x)$ denotes the box containing position x.

3. A Variance-reducing Technique

There are several techniques for reducing the variance in Monte Carlo calculations (see e.g. Hammersley and Handscomb, 1964), and at least one of these, the method of control variates, can be useful in the applications we study. (The variance is here defined as a measure of the statistical fluctuations, or, to be more precise, as the squared standard deviation of the results of similar calculations with different sets of random numbers.)

It is always desirable to minimize the importance of the randomly fluctuating variables in a system simulated with a Monte Carlo technique, and this is the essence of the control variates method. It may thus be advantageous *not* to let the model photons represent the radiation field itself, but rather the difference between the true field and a continuous radiation field. This is the case for instance if the excitation temperature in an optically thick transition varies only moderately throughout the region. The radiation temperature T_{ref} of the "reference" field may then be chosen as an approximate mean of the excitation temperature in the region. Alternatively, one might use the excitation temperature in those parts where the optical depth from the surface is near unity, i.e. where the line core is formed.

If a reference field is included, we must use the following equation instead of Eq. (1) when determining the number of model photons to be emitted in the various boxes:

$$N_r^{\text{diff}}=\left\{n_u-n_l\frac{g_u}{g_l}\exp\left(-h\nu_{ul}/kT_{\text{ref}}\right)\right\}A_{ul}. \tag{12}$$

If T_{ref} exceeds the excitation temperature in a box, N_r^{diff} will be negative here, as will be the weight of the model photons emitted within this box. Any difference between the true background radiation field and the reference field must be represented by a number of model photons entering the region from the outside; their weight will be negative if T_{ref} exceeds the radiation temperature of the background radiation.

The weight, here called W^{diff}, of a model photon must now be considered as the difference between the weight W^{true} of a model photon representing the true radiation field and the weight W^{ref} of one representing the reference field. The initial result of an emission within the region is a model photon with weight $W_0^{\text{diff}}=W_0^{\text{true}}-W_0^{\text{ref}}$. Eqs. (1) and (12) give the following relation between W_0^{true} and W_0^{diff}:

$$\frac{W_0^{\text{true}}}{W_0^{\text{diff}}}=n_u/\left\{n_u-n_l\frac{g_u}{g_l}\exp\left(-h\nu_{ul}/kT_{\text{ref}}\right)\right\}. \tag{13}$$

Similar reasoning holds for the model photons entering from the outside.

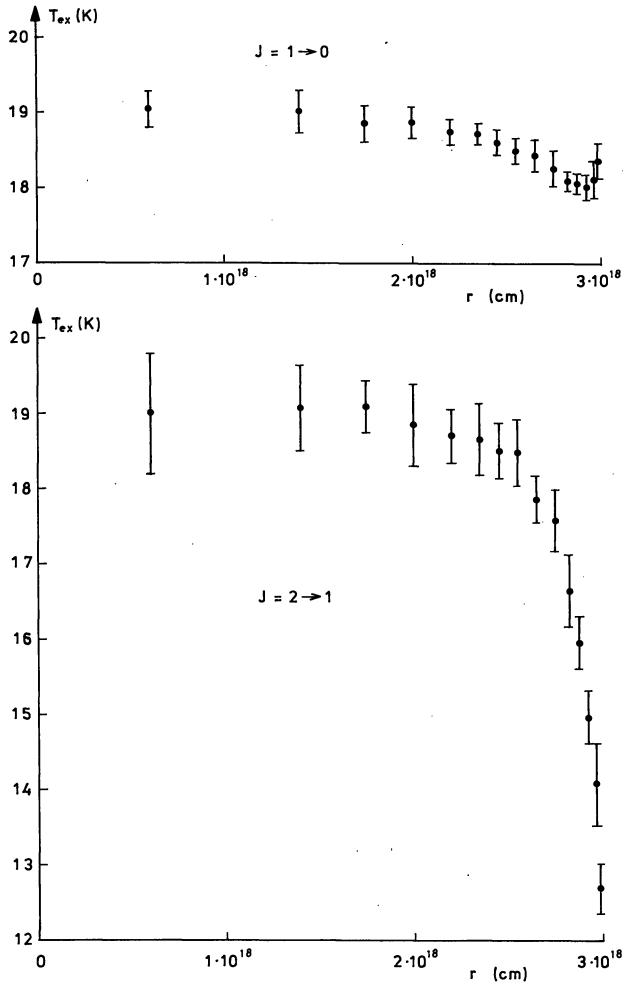

Fig. 1. The excitation temperature (T_{ex}) in the $J=1\rightarrow0$ and $J=2\rightarrow1$ CO transitions. The temperatures are plotted at positions (given by the distance r from the cloud centre) halfway between the inner and outer radii of the shell in question. The error bars show the standard deviations of the individual results of the 10 similar runs that were made with different random numbers

During the first step, the weight $W^{\rm diff}(x)$ varies as $W_0^{\rm true}\exp(-\tau_1 x/s_1) - W_0^{\rm ref}\exp(-t_1 x/s_1)$. t_1 is the optical depth along the first step that would be obtained if the excitation temperature were equal to $T_{\rm ref}$, i.e.

$$t_1 = \frac{h\nu_{ul}}{4\pi}\,\phi(\nu)\,n_{l,m}B_{lu}\,\{1-\exp(-h\nu_{ul}/kT_{\rm ref})\}\,s_1\,. \tag{14}$$

Hence, we must replace Eq. (5) by the following equation:

$$S^{\rm diff}_{lu,m} = \frac{h\nu_{ul}}{4\pi}\,\phi(\nu)\,B_{lu}\,\frac{s_1}{V_m}\left[\frac{W_0^{\rm true}}{\tau_1}\{1-\exp(-\tau_1)\} - \frac{W_0^{\rm ref}}{t_1}\{1-\exp(-t_1)\}\right]. \tag{15}$$

Eq. (6) is changed in analogy to this.

The statistical equilibrium equation in the two-level case will be

$$n_l[B_{lu}B(\nu_{ul},T_{\rm ref}) + \Sigma\, S^{\rm diff}_{lu,m} + C_{lu}] = n_u\left[A_{ul} + \frac{g_l}{g_u}\{B_{lu}B(\nu_{ul},T_{\rm ref}) + \Sigma\, S^{\rm diff}_{lu,m}\} + C_{ul}\right], \tag{16}$$

where $B(\nu,T)$ is the Planck function.

It should be realized that this is a very simple application of the control variates method, and that it may be possible to achieve even better results with modifications of this and other variance-reducing techniques.

4. The Monte Carlo Procedure Applied

Molecular line radiation in interstellar clouds is one obvious field of study where the Monte Carlo procedure described in the previous sections may be successfully used. The transfer of carbon monoxide (CO) line radiation in static dark clouds has been thoroughly treated by Leung and Liszt (1976), who used "conventional" numerical techniques for a consistent non-LTE, multi-level analysis. Similar methods were used by Lucas (1976) and Leung and Brown (1977), who studied the effects of velocity fields on CO line profiles.

Here, the performance of the Monte Carlo procedure is investigated in a test case similar to those studied by Lucas. The model is a spherical, homogeneous region with more or less typical dark cloud characteristics: radius $3\,10^{18}$ cm ($\sim$1 pc), number density of hydrogen molecules $2\,10^3$ cm^{-3}, kinetic temperature 20 K, and microturbulence 1 km s^{-1}. The cloud is collapsing with a velocity proportional to the distance from the centre, being -1 km s^{-1} at the periphery.

The number density of ^{12}CO relative to the number density of H_2 is taken to be $5\,10^{-5}$. The six lowest rotational levels are included in the analysis. Collisions with H_2 and He are taken into account, the number density of the latter being 20% of that of H_2. The collisional transition probabilities used are those calculated by Green and Thaddeus (1976).

The spherical cloud model is divided into 15 concentric shells, that correspond to the general concept of boxes used in the previous sections. Tests have shown that this number of subdivisions is quite sufficient for accurate calculations of the radiation in the present model to be possible. The thickness of the shells is gradually decreased towards the surface, in order to cover in detail any excitation temperature variations in those outer parts of the cloud where the shapes of the line cores are determined.

The 2.7 K microwave background radiation is represented by model photons emitted at the cloud surface towards the interior and uniformly distributed in frequency over bands whose widths are 7.5 km s^{-1} in velocity units. Each of the bands covers a CO line.

The step lengths of the model photons were chosen to bring them from one shell boundary to the next along the path. However, the step length was not allowed to exceed $3\,10^{17}$ cm (10% of the cloud radius). Hence, the maximum difference of the systematic gas velocity (along the photon's direction) between the start and end points of one step was 0.1 km s^{-1}, which is about 10% of the Doppler width.

A few short, preliminary runs were used to determine approximate excitation temperatures (correct to within 1 or 2 K) in the shells. These temperatures were then taken as initial values in a run consisting of 40 iterations, each with 200 emissions of model photons representing the radiation in all five radiative transitions simultaneously. No reference field was included. The

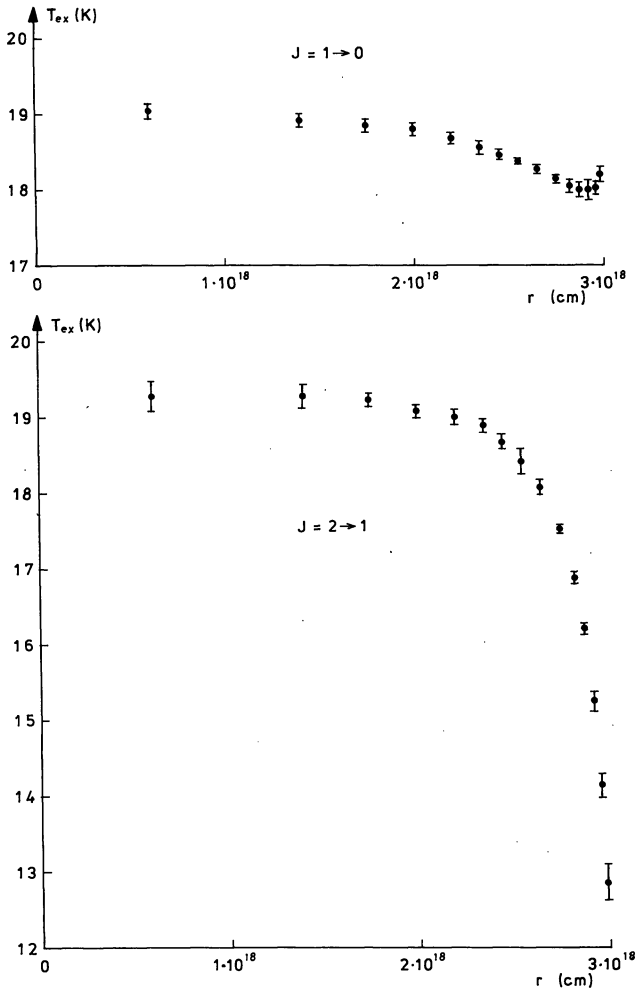

Fig. 2. Similar to Fig. 1, except that a reference radiation field was included in the calculation of the excitation temperatures to reduce the variance

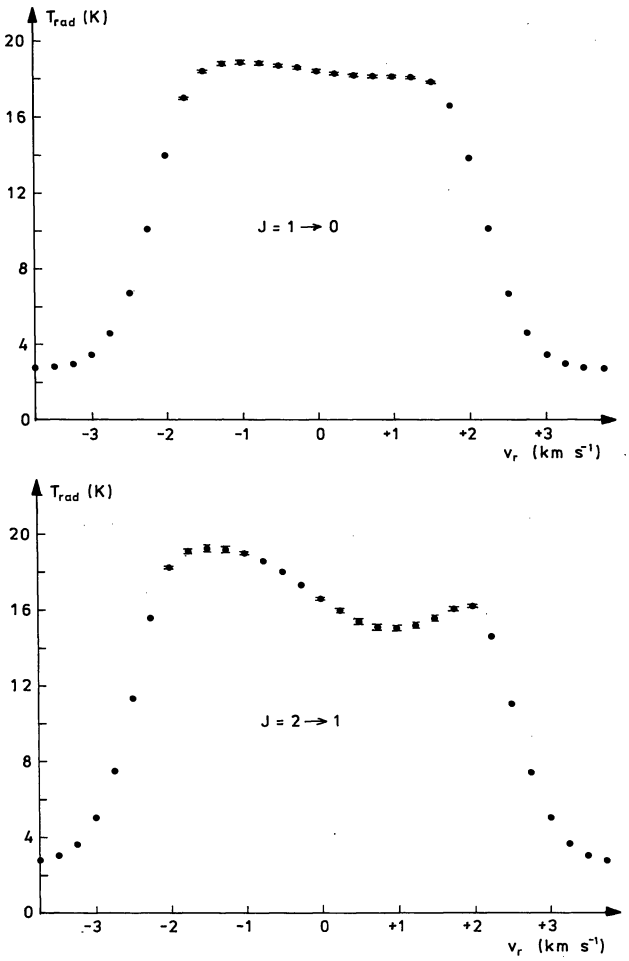

Fig. 3. Profiles of the $J=1\rightarrow0$ and $J=2\rightarrow1$ lines, based on the excitation temperatures shown in Fig. 2. The radiation temperature T_{rad} is given as a function of the radial velocity v_r relative to the velocity of the cloud centre, as seen by an observer outside the cloud. The error bars give the standard deviations of the individual results of the 10 runs

$\Sigma\, S_{lu,m}$ counters were emptied after iteration no. 10, and then again after iteration no. 20. The convergence achieved with this procedure was considered to be satisfactory, since the systematic differences between the results obtained with different choices of the initial excitation temperatures were smaller than the random noise. A total of 10 runs with the same initial excitation temperatures were made with different sets of random numbers, in order to get an idea of the scatter in the results. Figure 1 shows the obtained mean excitation temperatures for the transitions $J=1\rightarrow0$ and $J=2\rightarrow1$ in the 15 shells, with error bars showing the standard deviations of the individual values.

The whole procedure was then repeated with the variance-reducing method applied. The radiation temperature of the reference field (17 K at the $J=1\rightarrow0$ and $J=2\rightarrow1$ transitions) was chosen to minimize the energy carried by the model photons. Mean excitation temperatures with standard deviations obtained with 10 runs using the same initial excitation temperatures but different random numbers are shown in Fig. 2. Figure 3 shows the corresponding line profiles towards the cloud centre. These profiles were calculated for each of the runs separately, and the values in the figure are averages, with the standard deviations of the individual results shown in those parts of the profiles where they are large enough to be seen.

The line centre optical depth to the cloud centre is 6.0 and 15.5 in the $J=1\rightarrow0$ and $J=2\rightarrow1$ transitions respectively. Self-reversals are visible in both of the line profiles. These are caused by excitation temperature drops towards the cloud edges, where the optical depths from the surface are of the order 1 and less. However, the excitation temperature in the $J=1\rightarrow0$ transition does not fall very far below the kinetic temperature (20 K) where the optical depth from the cloud surface is small, and it even rises slightly in the outermost parts of the cloud. Hence, the self-reversal in the $J=1\rightarrow0$ line profile is quite insignificant compared to that in the $J=2\rightarrow1$ profile. The reasons for these conditions are the strong collisional coupling between the levels $J=0$ and $J=2$ and the rapid spontaneous deexcitation from $J=2$ to $J=1$. Near the boundary of the region, where the photons emitted in the $J=2\rightarrow1$ transition can escape from the cloud, this can lead

to an increased $J=1\rightarrow0$ excitation temperature (that may even under some circumstances exceed the kinetic temperature). Leung and Liszt (1976) describe this effect extensively.

As can be seen from Figs. 1 and 2, the standard deviations of the excitation temperatures become quite significantly smaller when the variance-reducing technique is included. In most parts of the cloud, the deviations are reduced typically by a factor of 2.5 in the $J=1\rightarrow0$ transition and a factor of 4 in the $J=2\rightarrow1$ transition, corresponding to a reduction of the computing time necessary to achieve a certain level of accuracy by factors of about 6 and 16, respectively. The better result in the latter case is due to the higher optical depth in the $J=2\rightarrow1$ transition – the continuous reference field is a better approximation to the true radiation field in this case.

As might be expected, the reduction is smaller in the outer parts of the cloud model, where the difference between the reference field and the true field is greater than in the interior. The higher noise in those outer shells where the core of the $J=2\rightarrow1$ line is formed is reflected by the relatively high standard deviations that can be found around frequencies corresponding to the radial velocity $+1$ km s^{-1} in the profile of this line.

A PDP 11/34 minicomputer with a 32 K memory but lacking a floating-point processor was used to obtain these results. Each run, during which 8000 model photons were emitted, took about 2.5 h. Much shorter computing times are possible with a faster computer – many common computers and minicomputers equipped with floating-point processors are a factor of 10–100 faster than the one used for these runs. For instance, the computing time was reduced to 5 min when the program was run on a CDC 6400.

The calculations described above were also carried out with separate model photon emissions in the various transitions (i.e. a total of 40,000 emissions during each run). In this case, however, the computing time was increased by about 75%, and the random noise was almost doubled.

Lucas (1976) used Rybicki's modification of the scheme developed by Feautrier to solve the radiative transfer equations. In order to get a quantitative comparison with his results, the Monte Carlo method was also applied to one of his models ($V_c=1$ km s^{-1}, $n_{H_2}=10^3$ cm^{-3}). The agreement between the results obtained with the two methods is very good over most parts of the line profiles – the difference is 2% or less in the line cores.

If judged solely on the basis of the computing time needed to achieve an accurate result, the Monte Carlo method cannot compete with the conventional method used by Lucas in the simple cases studied here. However, the simplicity and flexibility of the Monte Carlo program, the possibility to use a very small computer and the fact that an approximate solution can be calculated very rapidly should also be taken into account. Furthermore, the relative efficiency of the Monte Carlo approach increases quickly with the complexity of the investigated system, and this may well turn out to be its most valuable asset.

5. Conclusions

There are several reasons why the Monte Carlo method applied to radiative transfer problems should certainly not be disregarded as being slow and inaccurate. As shown above, the method can easily be used to solve non-LTE, multi-level problems under very general conditions – for instance, the inclusion of a velocity field of almost arbitrary scale and complexity can be accomplished with little more than an additional statement function in the program.

Since in general the number of steps that a model photon has to take depends on the number of subdivisions (boxes or shells) it crosses, the increase of the computing time necessary for a given accuracy with the number of subdivisions of the region under study is approximately linear. This, and the linear or slower than linear increase of the computing time with the number of transitions compares quite favourably with the properties of conventional numerical methods. Furthermore, no frequency or angular discretization is needed.

The Monte Carlo method is especially well suited for studies of the transfer of line radiation in stellar envelopes and interstellar clouds, where its ability to treat inhomogeneities and complex geometries is very useful. Difficulties will arise only if the optical depth is great – a rough practical upper limit of τ is 100.

Due to the square-root convergence that is unavoidable with this procedure, any method for reducing the variance will be of great value. It is shown that the control variates technique may be applied with considerable success, cutting down computing times typically by an order of magnitude in the calculation of CO line profiles in the dark cloud model that is discussed above. With this technique it was possible to reach a 1% or better accuracy in the calculated line profiles with a very reasonable amount of computing time.

Acknowledgements. It is a pleasure to thank Dr Bengt Gustafsson for the suggestion that Monte Carlo techniques may successfully be used to study non-LTE radiative transfer in the interstellar medium. My thanks are also due to him and to Dr Jan Askne, Steven Jörsäter, Dr R. Lucas, Dr Kalevi Mattila, Ingrid Melinder, Jesper Oppelstrup, Dr Kjell Rynefors, Dr Aage Sandqvist, and Göran Scharmer for generous help and fruitful discussions. Prof. Hans Wilhelmsson made the computer at the institution for electromagnetic field theory at the Chalmers University of Technology available for some initial test runs. Hans-Georg Gustavsson and Jan-Gunnar Tingsell helped me to make the acquaintance of this and other computers, and Bengt Greder drew the figures. Furthermore, I acknowledge the receipt of a doctoral fellowship from the University of Stockholm. This work was in part supported by the Swedish Natural Science Research Council.

References

Auer, L. H.: 1968, *Astrophys. J.* **153**, 783
Avery, L. W., House, L. L.: 1968, *Astrophys. J.* **152**, 493
Avery, L. W., House, L. L., Skumanich, A.: 1969, *J. Quant. Spectrosc. Radiat. Transfer* **9**, 519
Bernes, C.: 1978, Stockholm Observatory Report N° 15
Caroff, L. J., Noerdlinger, P. D., Scargle, J. D.: 1972, *Astrophys. J.* **176**, 439
Fleck Jr, J. A.: 1963, Methods in Computational Physics, Vol. 1, ed. Alder, B., Fernbach, S., Rotenberg, M., p. 43
Green, S., Thaddeus, P.: 1976, *Astrophys. J.* **205**, 766
Hammersley, J. M., Handscomb, D. C.: 1964, Monte Carlo Methods, Methuen, London
Holmlid, L., Rynefors, K. R.: 1978, *J. Comput. Phys.* **26**, 444
House, L. L., Avery, L. W.: 1969, *J. Quant. Spectrosc. Radiat. Transfer* **9**, 1579
Leung, C. M., Brown, R. L.: 1977, *Astrophys. J.* **214**, L73
Leung, C. M., Liszt, H. S.: 1976, *Astrophys. J.* **208**, 732
Lewis, P. A. W., Goodman, A. S., Miller, J. M.: 1969, *IBM Syst. J.* **8**, 136
Lucas, R.: 1976, *Astron. Astrophys.* **46**, 473

Magnan, C.: 1970, *J. Quant. Spectrosc. Radiat. Transfer* **10**, 1
Magnan, C.: 1972, *Astron. Astrophys.* **21**, 361
Modali, S. B., Brandt, J. C., Kastner, S. O.: 1972, *Astrophys. J.* **175**, 265
Modali, S. B., Brandt, J. C., Kastner, S. O.: 1975, *Astrophys. J.* **199**, 530
Price, M. J.: 1969, *Astrophys. Space Sci.* **4**, 182

Appendix

Pseudo-random numbers, uniformly distributed between 0 and 1, were obtained with the following algorithm:

$$S_n = 16807\ S_{n-1} (\mathrm{mod}\ 2147483647), \tag{A1}$$

$$R_n = S_n / 2147483647. \tag{A2}$$

R_n is the n:th random number, and S_n is an integer "seed". This pseudo-random number generator has been thoroughly tested by Lewis et al. (1969) and Holmlid and Rynefors (1978) and found to be satisfactory.

A uniform distribution between 0 and 1 of random numbers can be converted to other distributions with standard techniques described in any textbook on Monte Carlo methods, such as Hammersley and Handscomb (1964). With the formulae below those distributions that were needed for the present problem were obtained.

The following relation was used to select the distances r from the cloud centre where the model photon emissions took place:

$$r = \{r^3_{m,\,\mathrm{inner}} + R(r^3_{m,\,\mathrm{outer}} - r^3_{m,\,\mathrm{inner}})\}^{1/3}. \tag{A3}$$

Here, and below, R is a random number between 0 and 1 (obviously, a new random number was generated with Eqs. (A1) and (A2) whenever any of the formulae in this appendix was used to assign a value to a parameter). $r_{m,\,\mathrm{inner}}$ and $r_{m,\,\mathrm{outer}}$ are the inner and outer radii of the shell m where the model photon in question was emitted.

The isotropic distribution of the directions of those photons that were emitted within the cloud was achieved by assigning values to μ, the cosine of the angle between the photon direction and the outward radial direction, with

$$\mu = 1 - 2R. \tag{A4}$$

The distribution of frequency deviations, i.e. the Doppler profile $\phi(v)$, was simulated by means of Eq. (A5) below:

$$\Delta v = \sigma \sin(2\pi R)(-\ln R')^{1/2} + v(r)\mu \frac{v_{ul}}{c}. \tag{A5}$$

R and R' are two independent random numbers between 0 and 1, and $v(r)$ is the velocity in the outward radial direction of the gas at distance r from the cloud centre.

A correct distribution of μ for those model photons that entered the cloud from the outside was obtained with

$$\mu = -\sqrt{R}. \tag{A6}$$